



---

**Research Paper**

---

## **The Effects of Different Process Parameters of PLA+ on Tensile Strengths in 3D Printer Produced by Fused Deposition Modeling**

Faik YILAN<sup>1a</sup>, İbrahim Baki ŞAHİN<sup>1b</sup>, Fatih KOÇ<sup>2c</sup>, Levent URTEKİN<sup>1d</sup>

<sup>1</sup>Kırşehir Ahi Evran University, Engineering and Architecture Faculty, Mechanical Engineering Department, Kırşehir/ Turkey,

<sup>2</sup>Kırşehir Ahi Evran University, Engineering and Architecture Faculty, Metallurgy and Materials Engineering Department, Kırşehir/ Turkey  
[faik.yilan@ahievran.edu.tr](mailto:faik.yilan@ahievran.edu.tr)

**Received:** 23.09.2022

**Accepted:** 21.01.2023

**Abstract:** Fused Deposition Modeling (FDM) is a three-dimensional (3D) printing technique in which parts are produced with thermoplastic polymer layers in a highly controlled manner. However, the production of ready-made parts using FDM is quite tricky. At the same time, the mechanical properties of parts printed with current print parameters and low-cost 3D printers also vary. The quality and mechanical characteristics of the final part are influenced by production parameters such as the extrusion temperature, infill density, infill pattern, print speed, and layer height. This study focused on the effects of the infill pattern, infill density and print speed parameters on the tensile strength and production time of model structures printed with PLA+ material. A WDM-100E model, a tensile testing machine, has determined the tensile strength of the printed parts. In addition, the parts' tensile strengths and production times have been optimized by the signal-to-noise (SN) ratio analysis. The results reveal that the triangle infill pattern exhibits the best tensile strength at 40 mm/sec printing speed and 100% infill density. On the other hand, the lowest production time is observed in the gyroid infill pattern.

**Keywords:** Fused Deposition Modeling (FDM), PLA+, Infill Density, ANOVA

---

### **1. Introduction**

Manufacturing (production) is a basic requirement for improving people's quality of life and meeting their needs. At the same time, manufacturing as a result of human activities is a process that provides added value to the country's economy. The abundance, quality, variety and cheapness of production contributes positively to the country's economy and improves people's quality of life [1]. Due to the fact that existing resources have become insufficient, human beings have started to seek new resources to meet their needs. This search for new sources has brought along many different manufacturing technologies. In recent years, the additive manufacturing (AM) method, which is performed by three-dimensional printers, has come to the forefront among manufacturing methods, with the advantages of minimizing material waste and largely overcoming the geometric production restrictions [2]. Since the advent of 3D printing technology, known as rapid prototyping (RP) or AM, various 3D printing techniques have been developed [3–5]. Figure 1 shows the classification of these techniques into groups.

AM has applications in fields such as engineering, medicine, dentistry, automobile, aviation, architectonics, food and agriculture [4–8]. The expiration of old patents has made this technology more accessible [9]. In recent years, FDM, which is expressed by material extruding, has increased its popularity among AM technologies because of requires relatively less capital than other production technologies, ease of use and it can machine thermoplastic polymers such as ABS,

*How to cite this article*

Yılan, F., Şahin, İ.B., Koç, F., Urtekin, L. "The Effects of Different Process Parameters of PLA+ on Tensile Strengths in 3D Printer Produced by Fused Deposition Modeling" El-Cezerî Journal of Science and Engineering, 2023, 10(1); 160-173.  
ORCID ID: <sup>a</sup>0000-0001-7166-8604; <sup>b</sup>0000-0001-8090-9748; <sup>c</sup>0000-0002-4751-2340; <sup>d</sup>0000-0003-4348-4749

PLA, PC, PS, Nylon and PETG [10]. As a result of these developments, the costs of 3D printers have decreased significantly, their supply has become easier, and it has become possible to use them on a large scale in schools, homes, libraries and laboratories. During the coronavirus disease pandemic, the extensive manufacturing of 3D printed protection equipments has been an instance of this [11,12]. Since FDM technology was introduced by Scott Crump in 1988 this technology has developed greatly, reaching a level where everyone has a desktop 3D printer and can print parts with it [13,14]. Today, FDM has become the second most used 3D printing method after Stereolithography [15]. The FDM approach is based on the principle of facilitating the reshaping of the raw material (filament) by softening it with temperature. As it can be seen in Figure 2, the filament wound on the reel is pushed to the temperature-controlled nozzle by a gear mechanism, it melted there, and the intended model is obtained by pressing.

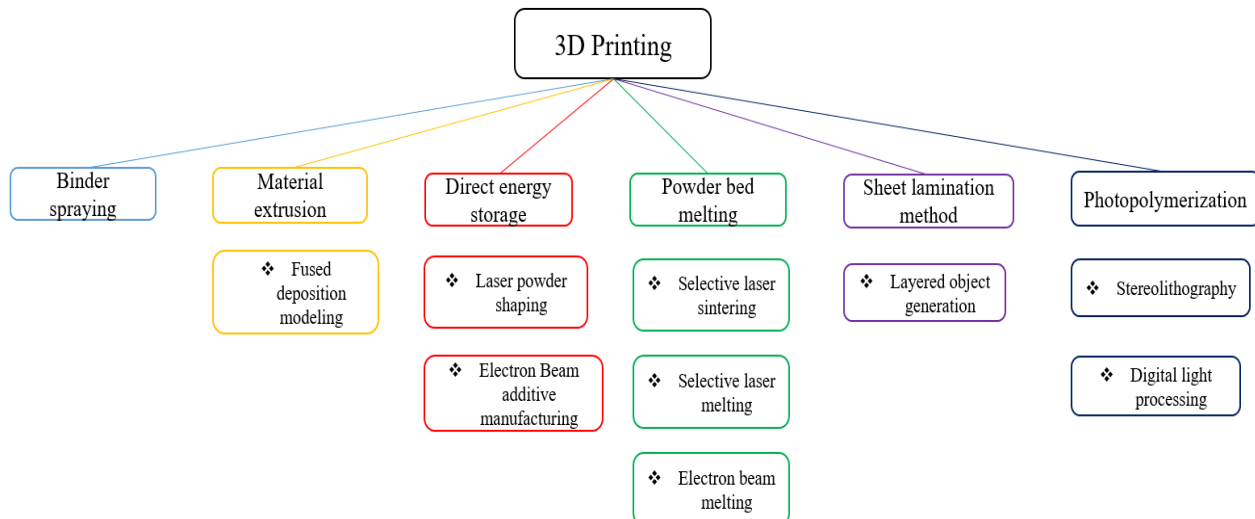


**Figure 1.** 3D printing types [3]

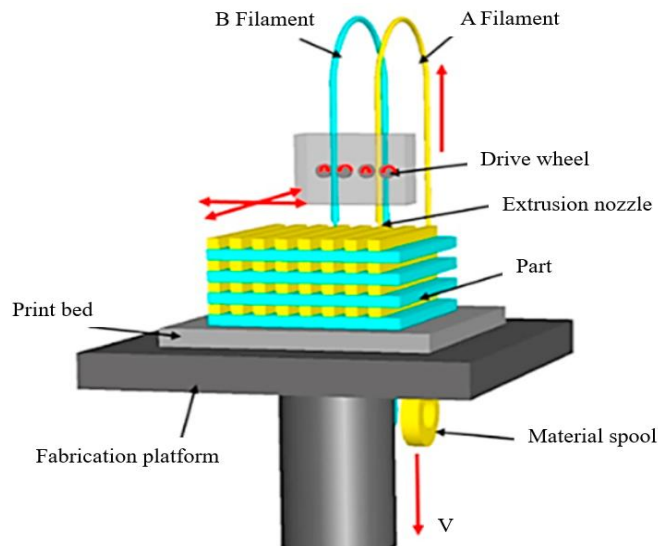


**Figure 2.** Schematic diagram of the FDM [9]

Fig. 3 shows the manufacturing workflow chart in FDM process. FDM starts with the design of the virtual part created in ".stl" format using computer-aided design (CAD) software such as FreeCAD, AutoDesig Inventor, Catia and SolidWorks etc. In the next step, this ".stl" file is converted into a file with the extension ".gcode", which the printer can process it, with another software (slicer). Printing parameters such as print speed, size, temperature, infill pattern, infill density, layer height and etc.

required to print the part are set in slicing programs such as Slic3r and Cura. In the last step, the file with the extension ".gcode" is uploaded to the printer, and the printing of the part is started [16,17].

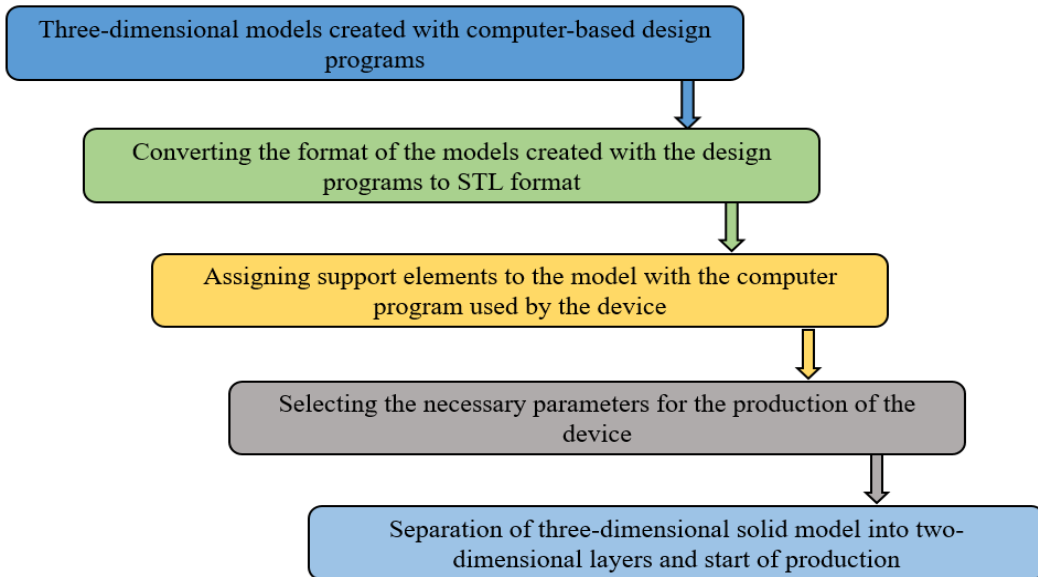


**Figure 3.** Process steps involved in 3D printing manufacturing [18]

As raw materials there are currently many filaments that can be used in FDM printing containing Polylactic acid (PLA), Acrylonitrile Butadiene Styrene (ABS), Polyvinyl Alcohol (PVA), Polyethylene Terephthalate Glycol (PETG), and each has different usage areas due to its different advantages and disadvantages. Among them, PLA is a biodegradable filament with a printing temperature of 160-230 °C and does not require a heated bed. In addition to these, its non-toxic nature, low cost, hard and strong structure have brought PLA to the forefront especially for biomedical applications. But at the same time, PLA is still a raw material open to development due to its fragile structure [19–23].

The mechanical characteristics of the final printed object are influenced by numerous FDM process parameters, as categorized in Table 1. Various process parameters such as nozzle temperature, volumetric flow rate, bed temperature, printing speed, infill density, layer height and wall thickness have been proven to be effective on the mechanical properties of the FDM-printed parts [24–26]. Therefore, a deeper understanding of the FDM process has a great importance in order to improve the mechanical properties of the printed material by adjusting the reasonable parameters.

**Table 1.** Settings for the 3D printing method [26]

Categories	Process parameters
Layer Formation	Print speed, Nozzle radius, Layer thickness, Feed rate, Raster angle.
Filling	Infill density, Air gap, Infill pattern.
Structure Orientation	Horizontal, Vertical, Transversal.
Temperature	Extrusion temperature, Ambient temperature.

In the literature, there are many studies on the effects of FDM process parameters on the mechanical properties of the produced material [27,28]. Popescu et al. [29] showed that process parameters such as raster-raster air gap, raster angle, layer thickness, infill density and structure orientation affect different mechanical properties such as tensile, compression and bending

strengths of the material. Gordilier et al. [30], emphasized that tensile strength can be maximized by combination of various process parameters. Ansari and Kamil [26] investigated the effects of printing speed and extrusion temperature on the dimensional quality and tensile strength of PLA. They observed that the dimensional deviation was lower at higher extrusion temperature and lower printing speed. However they obtained maximum tensile strength at high print speed. Günay et al. [31] investigated the effects of print speed, infill density and print direction parameters on the tensile strength of PLA+ sample and showed that infill density was the most effective parameter as a result of Taguchi analysis. Gonabadi et al. [32] evaluated the structure direction and infill density of PLA samples on their mechanical properties and emphasized that there was no effect on the tensile strength with the change of infill patterns. In addition to these, in the literature, there are studies focused on infill density and infill pattern parameters. Arjun et al. [33] reported that at 90% infill density the gyroid infill pattern showed the highest tensile strength in 20% carbon reinforced PLA test specimens. Also, Moradi et al. [34] using 6 different infill patterns in their study and obtained the highest tensile strength in the triangular pattern and the lowest tensile strength in the grid pattern. On the other hand, Akhoundi and Behravesh [35] investigated the effects of honeycomb, hilbert curve, concentric infill patterns on the tensile strength of PLA specimen and showed that the concentric infill pattern exhibited the highest tensile strength.

As it is seen from the relevant studies, effects different process parameters via FDM method on the mechanical properties of PLA materials are investigated in different studies. The main target of this study, the effects of infill density, infill pattern and print speed different parameters on the tensile strength of PLA+ specimens have been investigated. For this purpose, prepared PLA+ samples in ASTM D638 IV standard have been printed using the 3D printing device and then they have been subjected to tensile testing in the tensile device. The obtained results have been analyzed with the Taguchi approach and the most effective parameter has been tried to be determined.

## 2. Materials and Methods

### 2.1. 3D Device Design and Manufacturing

The samples produced for this study have been obtained with a 3D printer produced by us with a dual extrusion mechanisms, dual nozzles and 20x20x20 mm printing area. Arduino Mega 2560 physical programming platform and Ramps 1.6 3D printer control card have been used in the printer. A double-stepper motors have been used for z-axis in order to increase the z-axis precision. Since both nozzles reach high temperatures and cause blockages due to overheating of the heatsink in the dual nozzle structure, a second snail fan has been used to provide air flow under the heatsink. The design of the printer is given in Figure 4 and other technical details are given in Table 2.

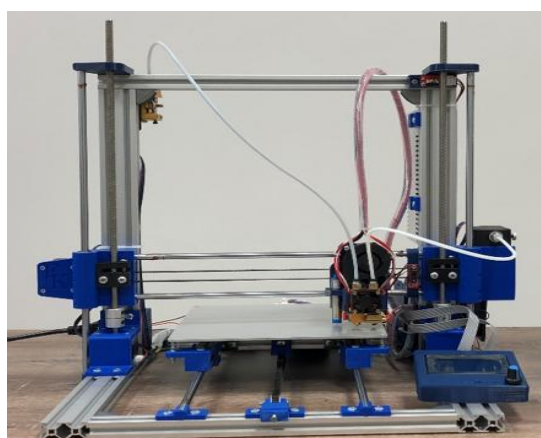


**Figure 4.** Manufactured 3D printer

**Table 2.** Details of the manufactured 3D printer [36]

Properties	
Print Area	20×20×20 mm
Material	PLA, TPU and PETG etc.
Table	Max. 140 °C heated
Print Speed	Max. 150 mm/s
Calibration	Automatic z-axis reset from 9 different points
Motion System	Linear shaft and screw shaft
Software	Open source
Working system	Cartesian
Structure	Aluminum sigma profile rigid structure

## 2.2. Material and Filament Properties

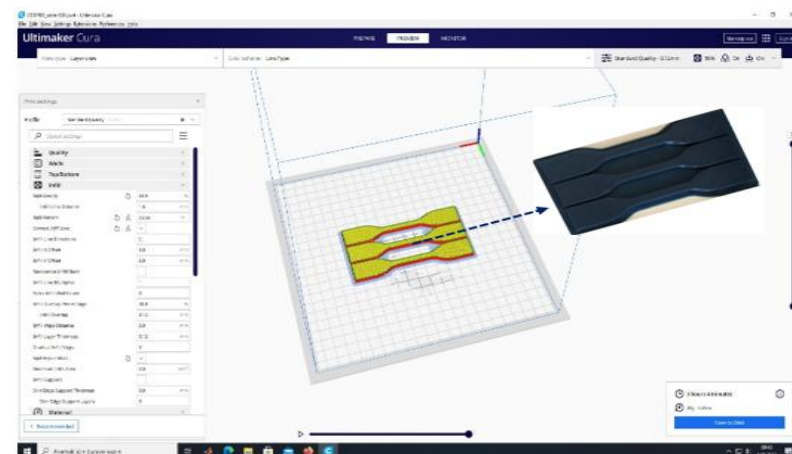
In this study, PLA+ filament has been used due to its increasing use in FDM printing processes and its environmentally friendly nature. The colour of the chosen filament is blue, and it has the diameter of 1.75 mm. Table 3 shows the properties of PLA+ materials according to ASTM D638 IV standard.

**Table 3.** Properties of PLA+ filament

Properties	Unit	Value
Shear Module	G	1287
Melting Temperature	°C	160-230
Poisson Ratio	θ	0.36
Elongation at Break	%	7
Yield Strength	MPa	70
Rockwell Hardness	Hr	88

## 2.3. Experimental Design

The technical drawing of the samples have been made with SolidWorks 2020 software according to ASTM D638 IV standards, and Ultimaker Cura software has been used as the slicer (Figure 5).

**Figure 5.** A sample inserted in Ultimaker Cura Software prior to slicing

The print speed parameter has been selected two levels, 40 mm/s and 60 mm/s. Three different geometric patterns octet, gyroid, and triangles have been used in the study (Figure 6). The layer height of the samples has been set at 0.12 mm. The three parameters examined in this experiment have been initialized with the L18 orthogonal array using the Taguchi Experimental Design method and the parameter values are tabulated in Table 4.

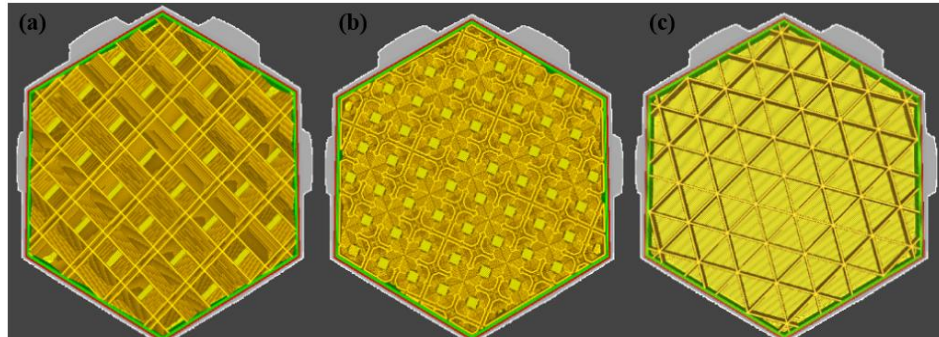


**Figure 6.** Schematic representation of infill patterns (a) Octet (b) Gyroid and (c) Triangles [37]

**Table 4.** Process parameters

Experiment number.	Infill patterns	Infill density (%)	Print speed (mm/sn)
1	Octet	100	60
2	Octet	100	40
3	Octet	75	60
4	Octet	75	40
5	Octet	50	60
6	Octet	50	40
7	Gyroid	100	60
8	Gyroid	100	40
9	Gyroid	75	60
10	Gyroid	75	40
11	Gyroid	50	60
12	Gyroid	50	40
13	Triangles	100	60
14	Triangles	100	40
15	Triangles	75	60
16	Triangles	75	40
17	Triangles	50	60
18	Triangles	50	40

## 2.4. Mechanical Test

### 2.4.1. Tensile Strength Test

The tensile strength tests of the specimens have been performed in Kırşehir Ahi Evran University Mechanical Engineering Department laboratory using a WDM-100E model tensile device (Figure 7). The maximum load capacity of the device is 100kN. The standards for producing tensile specimens on the FDM device have been selected ASTM D638 IV. The specimens were carefully clamped in the holders and tensile tests was performed. Deformation and load data are automatically recorded in a computer system. The test speed was kept as 0.50 mm/min for all the specimens as suggested by the test standard [38,39].

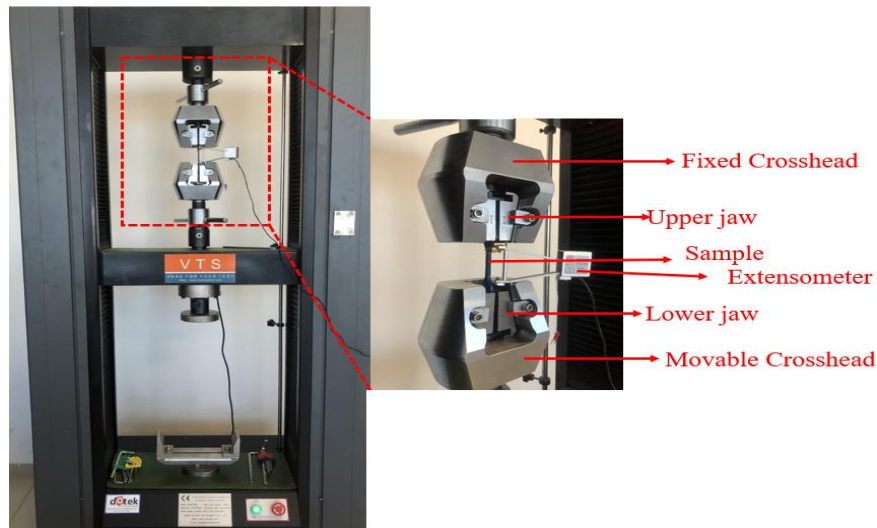


**Figure 7.** Tensile testing device (KAEU-Mechanical Engineering Mechanics Lab.)

The dimensions of the specimens subjected to the tensile test are given in Figure 8. For the tests, 3 samples have been produced for each combination of the infill pattern, infill density and print speed parameters given in Table 4, and the average of these 3 samples was taken as the test result. For this study, 36 specimens have been produced and tested. Figure 9 shows the deformed specimens after the tensile test.

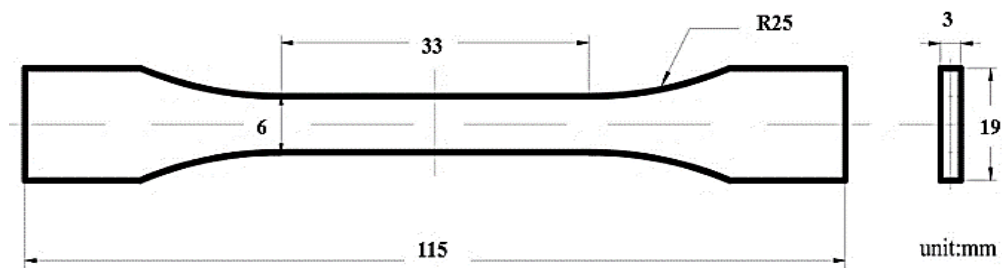


**Figure 8.** Design of tensile test specimen (according to ASTM D638 IV) [40]

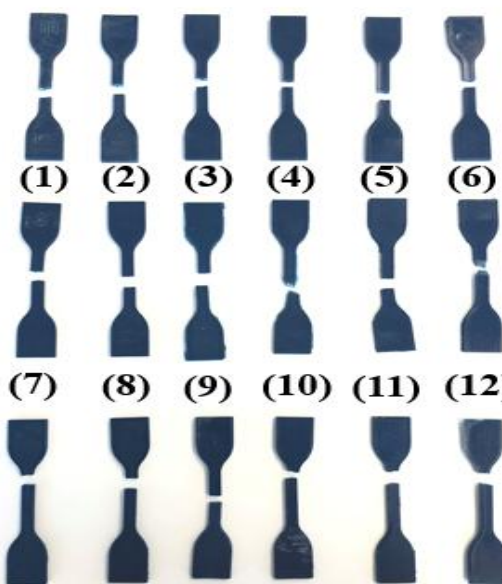


**Figure 9.** The 3D printed samples breaking off after tensile testing

### 3. Results and Discussion

In this study, ANOVA analysis has been imported into Minitab-19 software to decide how every entry factor contributed to the mechanical effects. The analysis of variance showing the percent contribution of each input parameter to the tensile strength is given in Table 5. It has been observed that the print speed and infill pattern have no direct effect on tensile strengths. In addition, it is possible to talk about the indirect effect of infill pattern and print speed on the infill density. On the other hand, the performed variance analysis for the production time is given in Table 6. The results of this analysis show that the most influential parameter on the production time is the print speed (46.4%), followed by the infill density (28.4%) and the infill pattern (8.7%). Production time and tensile strength signal-to-noise (S/N) ratio have been calculated under all experimental conditions (see Table 7). Considering the S/N ratio for tensile strength, “larger is better”, and for production time, the S/N ratio “smaller is better” type features.

**Table 5.** Variance table for tensile strength

Source	DF	Adj SS	Adj MS	F- Values	P- Values	Contribution (%)
Infill pattern	2	0,1651	0,0826	0,22	0,809	0,295953
Infill density (%)	2	50,6143	25,3071	66,04	0,000	90,72956
Print speed (mm/s.)	1	0,408	0,408	1,06	0,322	0,731368
Error	12	4,5985	0,3832	-	-	8,243122
Total	17	55,7859	-	-	-	100
<b>S =0,619036 R-Sq. =91,76 % R-Sq. (adj) =88,32%</b>						

**Table 6.** Variance table for production time

Source	DF	Adj SS	Adj MS	F- Values	P- Values	Contribution (%)
Infill pattern	2	2594800	1297400	3,17	0,078	8,704053
Infill density (%)	2	8477200	4238600	10,37	0,002	28,4361
Print speed (mm/s.)	1	13833800	13833800	33,84	0	46,4044
Error	12	4905600	408800	-	-	16,45545
Total	17	29811400	-	-	-	100
<b>S =639,375 R-Sq. =83,54 % R-Sq. (adj) =76,69%</b>						

Here, symbol A represents the infill density, and symbol B represents the print speed. These equations represent regression models for production time and tensile strength, respectively. When the equations are examined, it is understand that the infill density significantly affects both the production times and the tensile strengths. In Table 5 and Table 6, SS- represents sum of squares, DF- represents degrees of freedom, MS- represents the mean of squares, F- represents Fisers value, and P- represents probability. To accept the initial hypothesis that all means of the P-value are equal, we either assume it is equal to 0.05 or accepts it as less than 0.05. As a result, a P value of 0.809 confirms that the infill pattern signal factor has no significant effect on tensile strength. However, the F value, which represents a ratio between the variance of the whole group and the respective category groups, suggests that the infill density signal factor has a major effect on the tensile strength of 3D printed PLA+ test specimens. A Pareto chart with predictors of parameters is given in Figure 10.

**Table 7.** S/N ratios table

<b>Experiment no.</b>	<b>Production time (sn)</b>	<b>Tensile strength (MPa)</b>	<b>S/N ratios for production time</b>	<b>S/N ratios for tensile strength</b>
1	4560	12.175	-73,1793	21,7094
2	7200	12.2	-77,1466	21,7272
3	4020	8.1	-72,0845	18,1697
4	5340	8.125	-74,5508	18,1965
5	3600	7.67	-71,1261	17,6959
6	4560	8.7	-73,1793	18,7904
7	5400	11.4	-74,6479	21,1381
8	7320	11.675	-77,2902	21,3451
9	6000	8.65	-75,5630	18,7403
10	7140	9.2	-77,0740	19,2758
11	3600	8.42	-71,1261	18,5062
12	5400	8.075	-74,6479	18,1429
13	5400	11.425	-74,6479	21,1571
14	7320	12.55	-77,2902	21,9729
15	4020	9.775	-72,0845	19,8023
16	5340	9.65	-74,5508	19,6905
17	3600	7.4	-71,1261	17,3846
18	6360	7.55	-76,0691	17,5589

The developed regression models are given as

$$\text{Tensile Strength (MPa)} = 4,42 + 0,07870 * A - 0,0151 * B \quad (1)$$

$$\text{Production Time (s)} = 767310 + 33,60 * A - 87,7 * B \quad (2)$$

All the terms that crossed the reference line at 2.16 are significant at an alpha value of 0.05. Figure 10a illustrates that tensile strength; infill density is the most influential factor, followed by print speed. Accordingly, for production time, as shown in Figure 10b, the most influential factors are infill density followed print speed. Therefore, as shown from figure while the printing speed affects the production times, the infill pattern has a little effect on the production times and tensile strengths. The most important parameter affecting the tensile strength is the infill density. The main effect graph shows the S/N ratio, which affects the tensile strength and production time (Fig. 11 a-b).

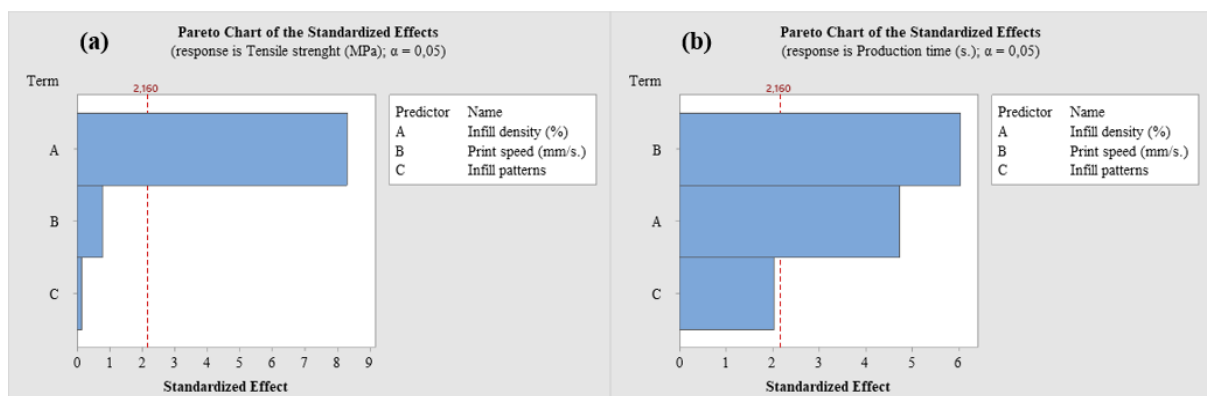


**Figure 10.** Pareto plot for PLA+ samples with predictors (a) tensile strength and (b) production time

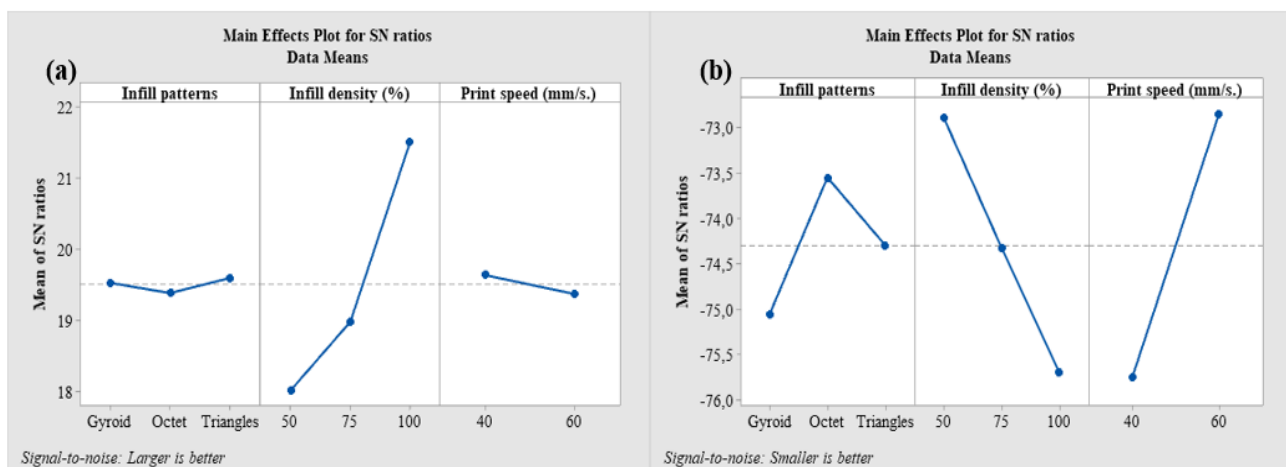


**Figure 11.** The main effect plot for the S/N ratio (a) tensile strength and (b) production time

As seen in the figures, the maximum tensile strength can be obtained with the triangle infill pattern, 100% infill density and 40 mm/sec printing speed parameters. When it comes to production time, ideal production time is achieved with gyroid infill pattern, 100% infill density and 40 mm/sec print speed parameters. The main effect graph on the infill density tensile strength, it is observed that the deviation increases with the increase of the filling density from 50% to 100%, while the deviation decreases with the increase of the printing speed from 40 mm/sec to 60 mm/sec. The interaction graphs are the graphical representation of the correlation between the infill density and infill pattern in terms of tensile strength and print time parameters (Fig. 12 a-b).

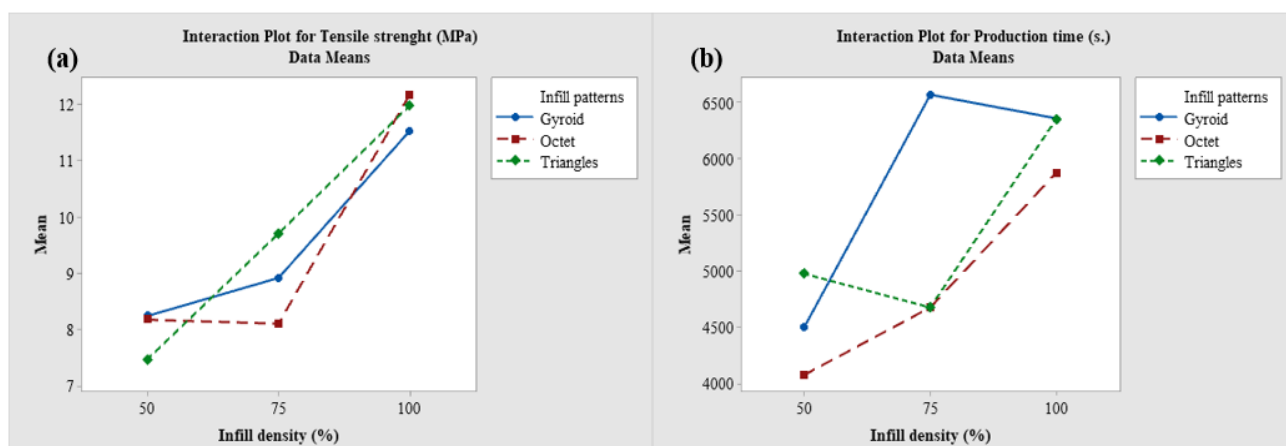


**Figure 12.** Interaction graph between infill density and geometric pattern (a) tensile strength and (b) production time

The averages of the datas for the PLA+ 3D-printed test specimens reveal a correlation with the ANOVA results, and a similarity is observed between the graphs for the infill density parameter. As can be seen from figures, the infill density has a bigger influence on the averages of the tensile strengths. It shows that at an infill density of 50% and infill pattern of triangles, the minimum mean is 7.5%; the octet and gyroid patterns it is approximately 8.2%. Figure 13 a-b indicate the influences of the infill density and print speed parameters on the production time and tensile strength. In terms of production time, the slower production time is obtained at low print speed and high infill density. Therefore, the production time can be reduced by increasing the printing speed. On the other hand, paying attention to Table 7, it is seen that higher tensile strength is obtained for the octet infill pattern at a 50% infill density than at a 75% infill density of the same pattern. It can be said that, the underlying reason of this situation is the octet infill pattern creates an inhomogeneous filling structure through the tensile direction.

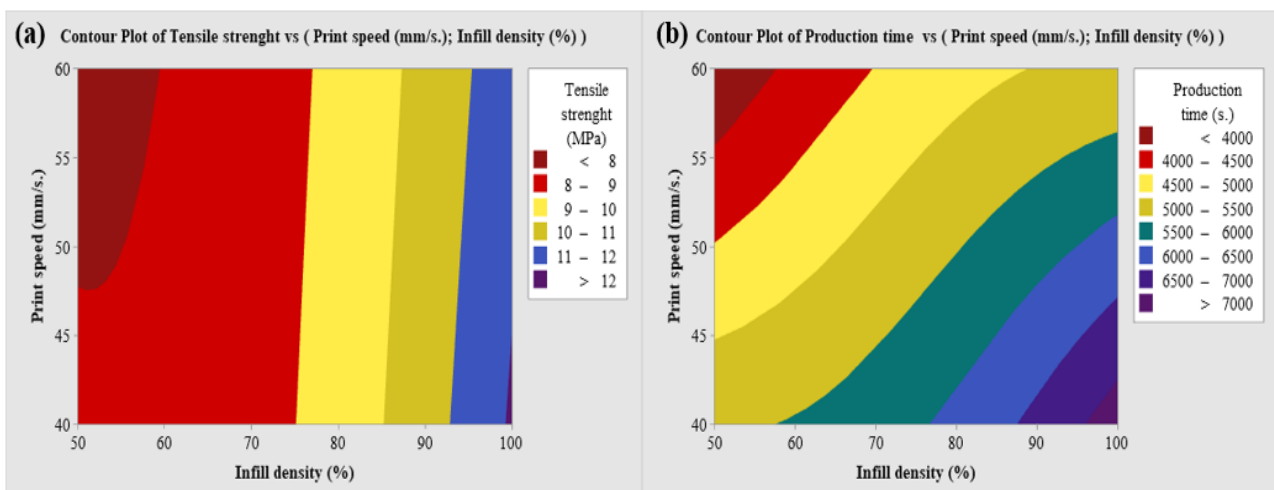


**Figure 13.** Contour plot (a) tensile strength and (b) production time

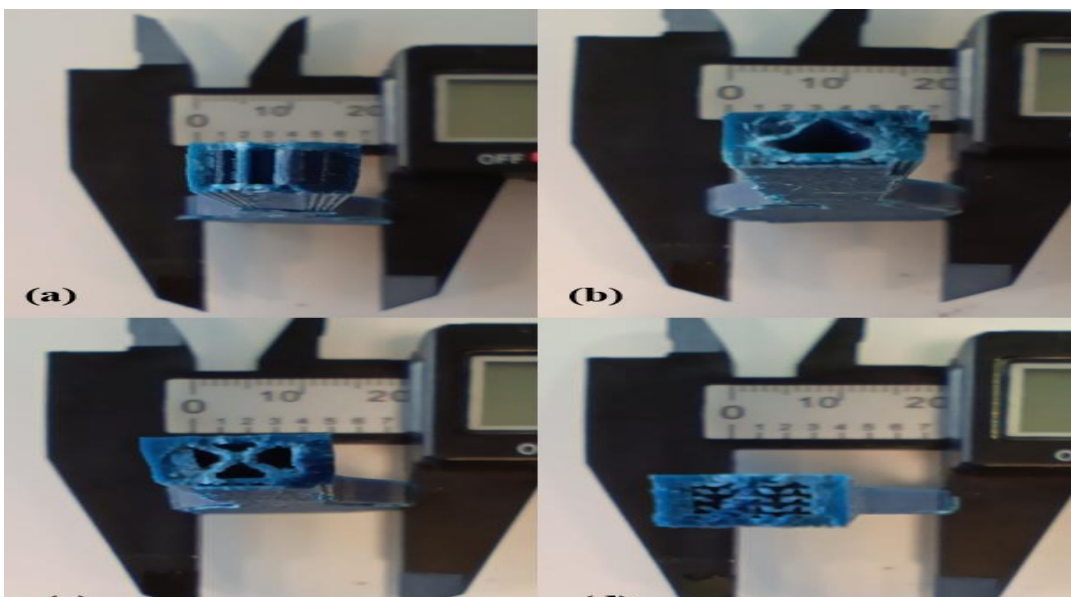


**Figure 14.** Cross-sectional views of infill patterns (a) octet 75%, (b) octet 50%, (c) triangles 75% and (d) gyroid 75%

As seen in Figure 14, at infill density of 50% the octet infill pattern left the middle of the sample, forming the pattern more homogeneously in the wall regions. However, at infill density of 75%, the octet geometric pattern created density in a certain region and left the other region empty. As a result of this, in the tensile strength tests, since the sample has been suffered premature rupture from

the weak region of the walls, lower tensile strengths has been obtained despite the high infill density. When it comes to the other infill designs, a homogeneous distribution was obtained in all filling ratios in the tensile direction, result of this no such unexpected results have been encountered.

#### 4. Conclusion

In this study, the influence of infill density, infill pattern and print speed parameters on the tensile strength and production time of 3D printed PLA+ samples, and the following results have been obtained as a result of the analysis:

- The production time has been affected by the printing speed of 46.4% and the filling density of 28.4%, respectively. The infill pattern has an effect of 8.7%. In this respect, although it has been determined in the analysis that the infill pattern does not affect the tensile strength, it can be mentioned that the effect of the infill pattern on the ratio of the infill density. Faster production time has been obtained in the gyroid infill pattern, 40 mm/sec print speed and 100% infill density.
- It has been determined that the most effective input parameter on the tensile strength is the infill density, with a rate of 90.7%, while the effect of other input parameters are smaller.
- It has been observed that the infill density significantly affects the tensile strength of 3D printed PLA+ specimens. The dense filled structure provides more strength. The best tensile strength have been obtained with triangles infill pattern, 100% infill density and 40 mm/sec print speed. In other words, as the infill density decreases, the tensile strength decreases.

It is recommended to examine the process parameters further to provide better control over the printed PLA+ parts by obtaining superior mechanical properties with good print quality.

#### Acknowledgment

This work; It was supported by Kırşehir Ahi Evran University Scientific Research Projects Coordination Unit with the project number MMF.A4.21.007. The authors of this study would like to thank KAUE-BAP for their support.

#### Authors' Contributions

FY contributed to the literature study, experimental study, device design, and writing of the article. İBŞ contributed to the analysis of the results and writing of the article. FK contributed to determining the subject and scope, determining the original value, designing the device, manufacturing and writing the text of the article. LU contributed to the writing of the article and the interpretation of the results. All authors have approved the final version of the article.

#### Competing Interests

The authors declare that they have no competing interests.

#### References

- [1]. Groover, M. P., Part II Engineering Materials. Fundam Mod Manuf Mater 2010:98–132.
- [2]. Gibson, I., Rosen, D., Stucker, B., Directed Energy Deposition Processes. In: Additive

- Manufacturing Technologies. 2015.
- [3]. Dizon, J. R. C., Espera, A. H., Chen, Q., Advincula, R. C., "Mechanical characterization of 3D-printed polymers", *Addit Manuf* 2018, 20: 44-67.
  - [4]. Stansbury, J. W., Idacavage, M.J., "3D printing with polymers: Challenges among expanding options and opportunities", *Dent Mater*, 2016, 32: 54-64.
  - [5]. Agrawaal, H., Thompson, J. E., "Additive manufacturing (3D printing) for analytical chemistry", *Talanta Open* 2021, 3: 100036.
  - [6]. Berman, B., "3-D printing: The new industrial revolution", *Bus Horiz*, 2012, 55: 155-62.
  - [7]. Murr, L. E., "Frontiers of 3D Printing/Additive Manufacturing: from Human Organs to Aircraft Fabrication", *J Mater Sci Technol.*, 2016, 32: 987-95.
  - [8]. Lille, M., Nurmiela, A., Nordlund, E., Metsä-Kortelainen, S., Sozer, N., "Applicability of protein and fiber-rich food materials in extrusion-based 3D printing", *J Food Eng.*, 2018, 220: 20-7.
  - [9]. Ngo, T. D., Kashani, A., Imbalzano, G., Nguyen, K. T. Q., Hui, D., "Additive manufacturing (3D printing): A review of materials, methods, applications and challenges", *Compos Part B Eng*, 2018, 143: 172-96.
  - [10]. Wang, S., Ma, Y., Deng, Z., Zhang, S., Cai, J., "Effects of fused deposition modeling process parameters on tensile, dynamic mechanical properties of 3D printed polylactic acid materials", *Polym Test* 2020, 86: 106483.
  - [11]. Oladapo, B. I., Ismail, S. O., Afolalu, T. D., Olawade, D. B., Zahedi, M., "Review on 3D printing: Fight against COVID-19", *Mater Chem Phys.*, 2021, 258: 123943.
  - [12]. Tino, A., Collange, C., Seznec, A., "SIMT-X: Extending Single-Instruction Multi-Threading to Out-of-Order Cores", *ACM Trans Archit Code Optim.*, 2020, 17.
  - [13]. Parandoush, P., Lin, D., "A review on additive manufacturing of polymer-fiber composites", *Compos Struct.*, 2017, 182: 36-53.
  - [14]. Gupta, M. K., Mia, M., Pruncu, C. I., Kapłonek, W., Nadolny, K., Patra, K., et al., "Parametric optimization and process capability analysis for machining of nickel-based superalloy", *Int J Adv Manuf Technol.*, 2019, 102: 3995-4009.
  - [15]. Bekas, D. G., Hou, Y., Liu, Y., Panesar, A., "3D printing to enable multifunctionality in polymer-based composites: A review", *Compos Part B Eng*, 2019, 179: 107540.
  - [16]. Latif, U., Pengaruh Dan Peran, "Media" Terhadap Siklus Penerapan Nilai-Nilai Dakwah Di Era Digitalisasi. At-Taujih Bimbing Dan Konseling Islam, 2021, 4: 1.
  - [17]. Buckner, C. A., Lafrenie, R .M., Dénommée, J. A., Caswell, J. M., Want, D. A., Gan, G. G., et al., We are IntechOpen , the world's leading publisher of Open Access books Built by scientists, for scientists TOP 1 %. Intech, 2016, 11:13.
  - [18]. Cano-Vicent, A., Tambuwala, M. M., Hassan, S. S., Barh, D., Aljabali, A. A. A., Birkett, M., et al., "Fused deposition modelling: Current status, methodology, applications and future prospects", *Addit Manuf.*, 2021, 47.
  - [19]. Jadhav, H., Jadhav, A., Takkalkar, P., Hossain, N., Nizammudin, S., Zahoor, M., et al., "Potential of polylactide based nanocomposites-nanopolysaccharide filler for reinforcement purpose: a comprehensive review", *Journal of Polymer Research*, 2020, 27: 1-36.
  - [20]. Li, G., Aspler, J., Kingsland, A., Cormier, L., Zou, X., "3D printing - A review of technologies, market and opportunities for the forestry industry", *Fibre Value Chain Conf Expo 2015 Pulp Pap Bioenergy Bioprod*, 2015, 5: 55-63.
  - [21]. Fehri, S., Cinelli, P., Coltell, M-B., Anguillesi, I., Lazzeri, A., "Thermal Properties of Plasticized Poly (Lactic Acid) (PLA) Containing Nucleating Agent", *Int J Chem Eng Appl.*, 2016, 7: 85-8.
  - [22]. Mrugalska, B., Trzcielinski, S., Karwowski, W., Nicolantonio, M. Di., "Advances in Intelligent Systems and Computing 1216 Advances in Manufacturing", *Production Management and Process Control Proceedings of the AHFE 2020 Virtual Conferences on Human Aspects of Advanced Manufacturing*, Advanced. 2020.

- [23]. Sakthivel, N., Bramsch, J., Young, P., Swink, I., Averick, S., Vora, H. D., "Investigation of 3D-printed PLA-stainless-steel polymeric composite through fused deposition modelling-based additive manufacturing process for biomedical applications", *Med Devices Sensors*, 2020, 3: 1-21.
- [24]. Yang, T. C., Yeh C. H., "Morphology and mechanical properties of 3D printed wood fiber/polylactic acid composite parts using Fused Deposition Modeling (FDM): The effects of printing speed", *Polymers (Basel)*, 2020, 12: 1334.
- [25]. Riddick, J. C., Haile, M. A., Wahlde, R Von, Colei, D. P., Bamiduro, O., Johnson, T. E., "Fractographic analysis of tensile failure of acrylonitrile-butadiene-styrene fabricated by fused deposition modeling", *Addit Manuf.*, 2016, 11: 49-59.
- [26]. Ansari, A. A., Kamil, M., "Effect of print speed and extrusion temperature on properties of 3D printed PLA using fused deposition modeling process", *Mater Today Proc.*, 2021, 45: 5462-5468.
- [27]. Torres, J., Cole, M., Owji, A., DeMastry, Z., Gordoni A. P., "An approach for mechanical property optimization of fused deposition modeling with polylactic acid via design of experiments", *Rapid Prototyp J.*, 2016, 22: 387-404.
- [28]. Rao, R. V., Rai, D. P., "Optimization of fused deposition modeling process using teaching-learning-based optimization algorithm", *Eng Sci Technol an Int J.*, 2016, 19: 587-603.
- [29]. Popescu, D., Zapciu, A., Amza, C., Baciu, F., Marinescu, R., "FDM process parameters influence over the mechanical properties of polymer specimens: A review", *Polym Test*, 2018, 69: 157-166.
- [30]. Gordelier, T. J., Thies, P. R., Turner, L., Johanning, L., "Optimising the FDM additive manufacturing process to achieve maximum tensile strength: a state-of-the-art review", *Rapid Prototyp J.*, 2019, 25: 953-71.
- [31]. Günay, M., Gündüz, S., Yılmaz, H., Yaşar, N., Kaçar, R., "PLA Esaslı Numunelerde Çekme Dayanımı İçin 3D Baskı İşlem Parametrelerinin Optimizasyonu", *J Polytech*, 2020, 23(1): 73-79.
- [32]. Gonabadi, H., Yadav, A., Bull, S. J., "The effect of processing parameters on the mechanical characteristics of PLA produced by a 3D FFF printer", *Int J Adv Manuf Technol.*, 2020, 111: 695-709.
- [33]. Arjun, P., Bidhun, V. K., Lenin, U. K., Amritha, V. P., Pazhamannil, R. V., Govindan, P., "Effects of process parameters and annealing on the tensile strength of 3D printed carbon fiber reinforced polylactic acid", *Mater Today Proc.*, 2022, 62: 7379-7384.
- [34]. Moradi, M., Aminzadeh, A., Rahmatabadi, D., Hakimi, A., "Experimental investigation on mechanical characterization of 3D printed PLA produced by fused deposition modeling (FDM)", *Mater Res Express*, 2021, 8.
- [35]. Akhoundi, B., Behravesh, A. H., "Effect of Filling Pattern on the Tensile and Flexural Mechanical Properties of FDM 3D Printed Products", *Exp Mech.*, 2019, 59: 883-897.
- [36]. Yılan, F., Şahin, İ. B., Urtekin, L., "3D Printing Design and Manufacturing: Dual-Extrusion System", *New Trends Eng. Sci.*, *New Trends in Engineering Sciences*, 2022, 151-61.
- [37]. Infill setting [Internet]. Ultimaker Support. Ultimaker; 2020 [cited 2022 September 15] Available from: <https://support.ultimaker.com/hc/en-us/article/360012607079-Infill-settings>.
- [38]. Akdoğan, E., Şahbaz, M., "Tensile behavior of compressed high-density polyethylene materials", *Journal of Materials and Manufacturing*, 2022, 1(1): 1-6.
- [39]. Phillips, C., Kortschot, M., Azhari, F., "Towards standardizing the preparation of test specimens made with material extrusion: Review of current techniques for tensile testing", *Addit Manuf.*, 2022, 58: 103050.
- [40]. Erdoğan, B., Bağatur, M., Güngör, G., "Experimental investigation of tensile strength and thermal conductivity of nanoparticle reinforcement composite materials", *Journal of Materials and Manufacturing*, 2022, 14-21.